Original Article

Monte Carlo N Particle code - Dose distribution of clinical electron beams in inhomogeneous phantoms

H. A. Nedaie, M. A. Mosleh-Shirazi[1], M. Allahverdi[2]

Department of Radiotherapy Physics, Cancer Research Centre, Cancer Institute, Tehran University of Medical Sciences, Tehran, [1]Department of Radiotherapy, Radiotherapy Physics Unit, Namazi Hospital, Shiraz University of Medical Sciences, Shiraz, [2]Department of Nuclear Engineering, Shahid Beheshti University, Tehran, Iran

Received on: 07.08.12 **Review completed on: 10.11.12** **Accepted on: 14.11.12**

ABSTRACT

Electron dose distributions calculated using the currently available analytical methods can be associated with large uncertainties. The Monte Carlo method is the most accurate method for dose calculation in electron beams. Most of the clinical electron beam simulation studies have been performed using non- MCNP [Monte Carlo N Particle] codes. Given the differences between Monte Carlo codes, this work aims to evaluate the accuracy of MCNP4C-simulated electron dose distributions in a homogenous phantom and around inhomogeneities. Different types of phantoms ranging in complexity were used; namely, a homogeneous water phantom and phantoms made of polymethyl methacrylate slabs containing different-sized, low- and high-density inserts of heterogeneous materials. Electron beams with 8 and 15 MeV nominal energy generated by an Elekta Synergy linear accelerator were investigated. Measurements were performed for a 10 cm × 10 cm applicator at a source-to-surface distance of 100 cm. Individual parts of the beam-defining system were introduced into the simulation one at a time in order to show their effect on depth doses. In contrast to the first scattering foil, the secondary scattering foil, X and Y jaws and applicator provide up to 5% of the dose. A 2%/2 mm agreement between MCNP and measurements was found in the homogenous phantom, and in the presence of heterogeneities in the range of 1-3%, being generally within 2% of the measurements for both energies in a "complex" phantom. A full-component simulation is necessary in order to obtain a realistic model of the beam. The MCNP4C results agree well with the measured electron dose distributions.

Key words: Dose distribution, dosimetry, electron therapy, heterogeneous phantom, Monte Carlo N Particle

Introduction

Monte Carlo (MC) techniques are becoming more widely used in all medical physics applications. MC simulation of radiation transport is one of the most accurate methods for predicting absorbed dose distributions in radiation therapy. Electron dose distributions calculated using currently available analytical methods are associated with large uncertainties, especially in irradiated volumes that contain inhomogeneities such as air cavities and bones.[1,2] In clinically relevant dose calculations, errors of 10% or greater have been reported to be associated with analytic dose calculation methods.[3,4] The MC method is the most accurate method for dose calculation in electron beams and can potentially reduce these uncertainties to a few percent.[5-9] In particular, MC simulation can handle backscatter from high-density materials (such as bone) or scatter perturbations by air cavities more accurately than any other current dose calculation method.[5,10]

There are different MC codes for the simulation of photons, electrons and the coupled transport of electrons and photons. There are three main families of MC codes frequently used for the modeling of electron beams: Electron TRANsport/Integrated Tiger Series (ETRAN/ITS),[11,12] Electron Gamma Shower (EGS4),[13] and Penetration and ENErgy LOss of Positrons and Electrons (PENELOPE).[14] The MCNP code is based on the ETRAN/ITS electron transport system.

For electron transport, there are four main differences between MCNP and EGS-based codes; namely, secondary electron creation, multiple scattering theories, electron

Address for correspondence:
Dr. Hassan A. Nedaie,
Department of Radiotherapy Physics, Cancer Institute, Imam Hospital, Keshavarz Blvd., Tehran, Iran.
E-mail: Nedaieha@sina.tums.ac.ir

Access this article online	
Quick Response Code:	Website: www.jmp.org.in
	DOI: 10.4103/0971-6203.106607

step mechanics and cross-sections used. For creation of secondary electrons, MCNP uses a class I algorithm (for collisional energy loss), where the energy losses and angular deflections associated with all individual events are grouped together and the energy and direction of the primary electron are not affected by the creation of individual secondary particles.[15,16] On the other hand, EGS4 uses a class II algorithm, where the individual interactions affect the energy and direction of the primary electron when they create knock-on electrons or bremsstrahlung photons above certain energy thresholds, although the effects of secondary particle production below these thresholds are still grouped together. To calculate the elastic scattering angular deflections of an electron, MCNP uses the Goudsmit–Saunderson theory,[17] and EGS4 uses the Moliere theory. While the Goudsmit–Saunderson theory is valid for arbitrary angular deflections, the Moliere theory works well for small angular deflections only. Also, the cross-sections used in the multiple scattering theories are different in the two codes. For energies below 0.256 MeV, MCNP uses the cross-sections from numerical tabulations based on a partial wave expansion method. For higher energies, a combination of the Mott and Rutherford cross-section with a screening correction is used. The Moliere theory, on the other hand, is based on the screened Rutherford cross-section.

Most of the clinical electron beam simulation studies have been performed using non-MCNP codes.[18] Given the above-mentioned differences between the MC codes, this work aims to evaluate the accuracy of MCNP4C-simulated electron beam dose distributions in a homogenous phantom and in inhomogeneities for beams generated by a commercial linear accelerator.

Materials and Methods

Homogeneous phantom

A PTW water tank (PTW FRUIBURG, Freiburg, Germany) was used as a homogenous phantom for relative dosimetry. The phantom was a cube of dimensions 50 cm × 50 cm × 50 cm within which electron diodes (reference and detector) were placed in the radiation field for scanning. The acquired data were analyzed using the MEPHYSTO (PTW beam analyzer) software.

Heterogeneous phantoms

Different types of phantoms were made. The phantoms were polymethyl methacrylate (PMMA) slabs containing different-sized, low- and high-density inserts of heterogeneous materials. The materials chosen had linear collision stopping powers and linear angular scattering powers close to body tissues.[19] A PMMA frame was constructed to fit the top of the water tank in order to accommodate different-sized heterogeneous phantoms while allowing scans within water beyond the heterogeneities.

Phantom A ("ribs" equivalent phantom)

This phantom consisted of two 15-cm-long hard-bone rods with a diameter of 1 cm. They were inserted in a 20 cm × 20 cm × 2 cm PMMA slab. The center-to-center rib separation was 1.5 cm. The central axis of the radiation beam was centered between the ribs [Figure 1].

Phantoms B and C (air cavity and hard-bone equivalent phantom)

This phantom was a 20 cm × 20 cm × 2 cm PMMA slab with a 2 cm diameter, 1.8-cm-long cylindrically shaped hole in the center to represent an air cavity or accommodate a hard-bone insert (made of Teflon). The cylinder's axis was parallel to the beam's central axis and the top of the cylinder was recessed from the top of the slab by 2 mm. During air cylinder measurements, a thin layer of nylon was attached to the bottom surface of the phantom to prevent water from filling the hole [Figure 2].

Phantom D ("spine and trachea" equivalent phantom)

The aim of designing this phantom was to investigate the effect of bone and air inhomogeneities together on the electron beams (i.e., in a relatively complex 3D inhomogeneous phantom). The base of this phantom was a 30 cm × 30 cm × 4.9 cm PMMA slab. There was a long cylindrical hole (representing the trachea), with its long axis perpendicular to the central axis of the beam 2 mm below the top surface. The hole had a diameter of 3 cm. Five 1.2-cm-thick, 2.5 cm diameter hard-bone material disks were 0.5 cm below the trachea hole and their axes were parallel to the radiation beam central axis. The disks were separated 1.5 cm edge-to-edge. Because the applicator size was 10 × 10, the started scanned point was under 3rd Teflon disk. This phantom was used in the "trachea down" position and the beam was incident from the bone side of the phantom. This phantom was positioned above the PMMA frame on the surface of water [Figure 3].

Measurements

Electron beams with 8 and 15 MeV nominal energy generated by an Elekta Synergy linear accelerator were

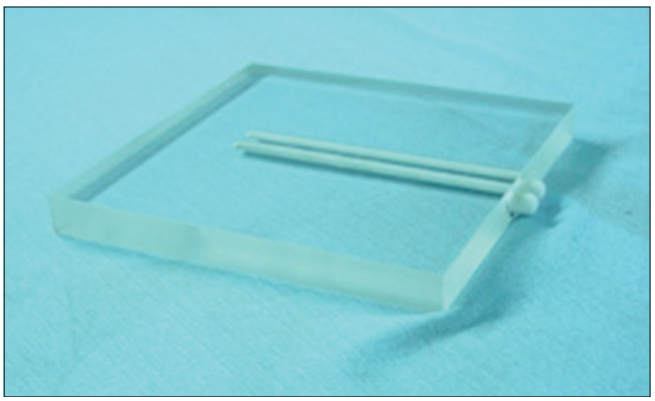

Figure 1: Picture of phantom A (rib slab)

used. Measurements were performed for a 10 cm × 10 cm applicator at a source-to-surface distance of 100 cm. Dose profile scans were obtained at 1 cm depth for both electron beams. All measurements were performed using a PTW water tank. The sensitive volume of the diode detector was 0.2-0.3 mm^3 and the sensitivity was 100 nC/Gy. For all measurement set-ups, we considered the diode's effective point of measurement located 0.5 mm below its surface.[20] The diode system was tested against ionization chambers for a limited set of measurements covering both the electron energies involved.

Simulation of the linear accelerator

Full MC simulation of the detailed geometry of the treatment head according to the manufacturer's data was used and two energies (8 and 15 MeV) and one applicator (10 cm × 10 cm) were chosen [Figure 4].[21] These energies are relevant in electron beam therapy and use different scattering filters in the linear accelerator. During simulation, the effect of each component on the 15 MeV central-axis electron percentage depth dose (PDD) was investigated.

Two methods were chosen to define the source: (a) Point source with monoenergetic electron beam and (b) extended electron source with radius of 0.5 and 0.6 mm for 8 and 15 MeV, respectively. The energy spectra with probability distribution were chosen, the mean energies of which were 8.3 and 15.3 MeV, respectively. Energy windows were ± 0.8 and ± 1.3 MeV, respectively. After benchmarking, the second source definition was preferred. All calculations were carried out in a coupled electron–photon mode [Mode PE]. Following Jeraj's work, the ITS energy-indexing algorithm was used for all main simulations by using the Debug Information card [DBCN 17J 1].[16,22] Electron and photon energy cut-offs were both set at 0.01 MeV.

Results

Homogeneous phantom

Tables 1 and 2 summarize the differences between the measured and the calculated (simulated) dose in PDD and profiles for both energies. The measurement data were extracted from Nedaie *et al.*'s work.[21] The discrepancies between measured and calculated dose data are within 2% of D_{max} and within 2 mm in the high-gradient regions for both 8 and 15 MeV energies.

The effect of individual head components

Figure 5 shows the PDD graphs for different cases in the study of the effect of individual components on PDD. Seven cases (denoted by letters A-G) were simulated for a 15 MeV electron beam to reflect increasing levels of complexity. An additional part of the beam-defining system was introduced into the simulation in each successive case. In case A, a monoenergetic pencil beam was incident directly on the phantom. In case B, a mononergetic beam with a 1° downward distribution at 100 cm from the phantom was used and the effect of intervening air was simulated. In case C, the degree of divergence was increased to 27°, corresponding to the real angle between primary collimators. Further parts were added in turn for the remaining cases. "Full component" includes the mylar screen and mirror in addition to the other components in case G.

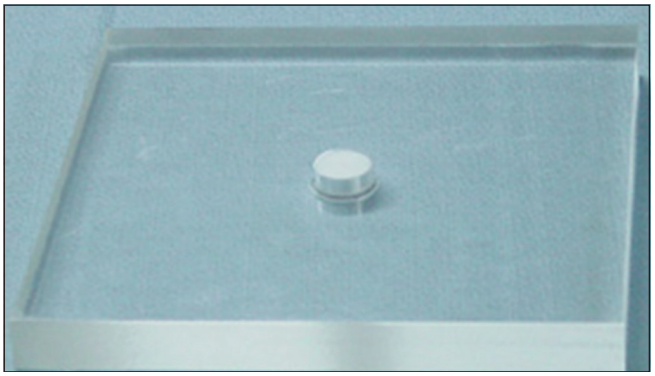

Figure 2: Picture of phantom B (hard bone slab) and phantom C (if take the Teflon disk)

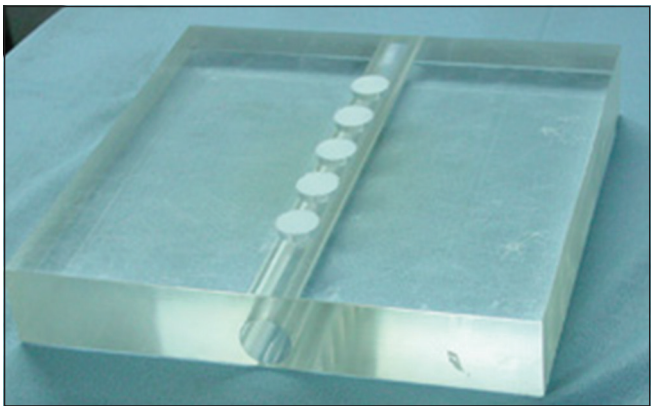

Figure 3: Complex geometry phantom in position trachea down (phantom D)

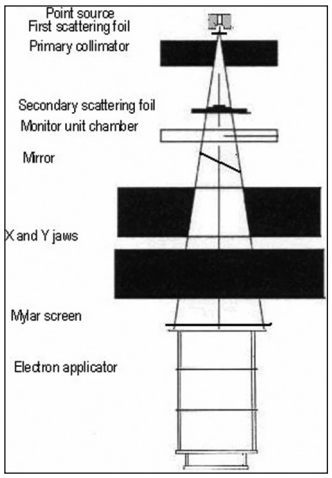

Figure 4: Detailed geometry of head component

Phantom A

Figures 6 and 7 show the comparisons between the measured and the MC-calculated dose profiles for phantom A at both 8 and 15 MeV electron beam energies. MC simulation was done for only ± 4 cm from the central axis in order to reduce run time. The statistical uncertainties are within 1-1.5%. The largest discrepancy between the measured and the calculated dose profile is less than 3% for the 8 MeV beam. The agreement for the 15 MeV beam is within 0.5-1% in most areas, but at the cold points, it is within 3%. The difference in mass scattering power between bone and water is larger for lower energy electrons than for higher energy. Scattered electrons from the two ribs contribute to the increase in dose (increase in electron fluence) laterally to each side of the rib and decrease in dose beyond the ribs (decrease in primary electron fluence). This scattering effect can be seen to be more severe for 8 MeV than for 15 MeV.

Table 1: Differences for measured and calculated percentage depth dose

Energy (MeV)	*Differences up to D_{max} (%)*	*Differences at D_{max} (mm)*	*Differences at 50% depth (mm)*	*Differences at bremesstralung tail %*
8	Within 1.2	0	1.7	0.4
15	Within 1.0	1.0	1.8	0.6

Table 2: Differences for measured and calculated beam profile

Energy (MeV)	*Differences at flat area %*	*Differences at 50% depth (mm)*	*Differences at bremesstralung tail %*
8	Within 1.0	1.8	0.2
15	Within 0.7	1.2	0.1

Phantom B

Figures 8 and 9 show the results of dose distributions beyond the air cavity at the depth of 1 cm under the inhomogeneity for the 8 and 15 MeV energies, respectively. In Figure 5, MCNP predicts a hot spot with about 50% dose enhancement immediately behind the small air cavity for the 8 MeV beam. For the 15 MeV beam, the agreement between measured and calculated doses is also remarkable because MCNP can predict the very fine details of the dose profile at a depth of 1 cm under the inhomogeneity [Figure 10]. The agreements are approximately within 1.5% and 1% for the 8 MeV and 15 MeV electron beams, respectively. The MCNP dose

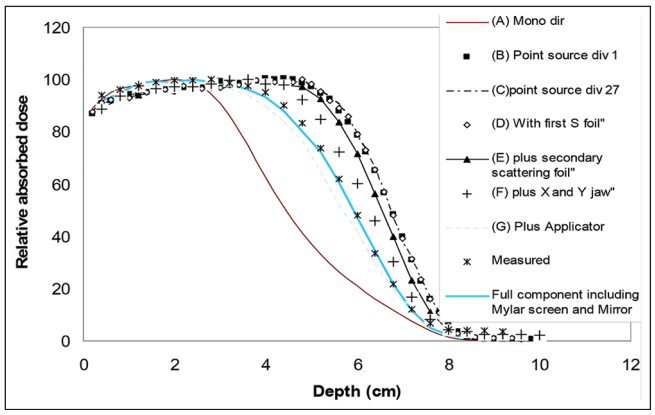

Figure 5: The effects of different individual linear accelerator head components on a 15 MeV electron beam percentage depth dose

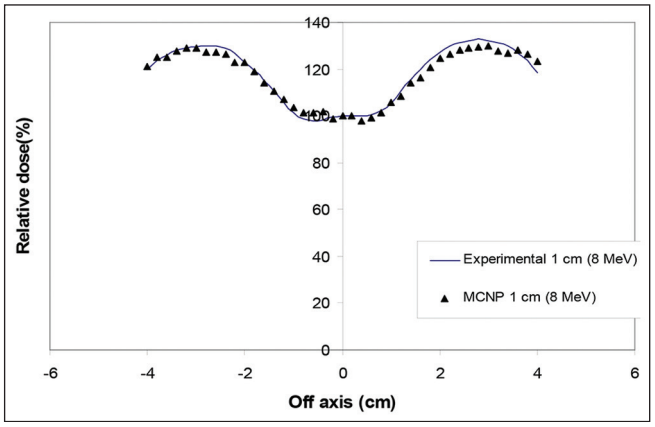

Figure 6: Measured and calculated doses for the 8 MeV beam with phantom A at the plane 1 cm below the ribs slab

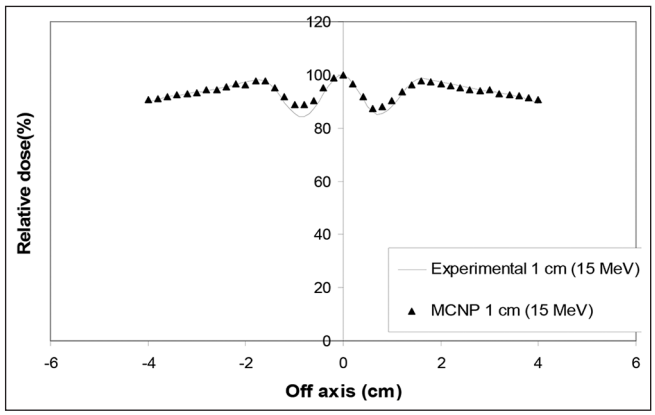

Figure 7: Measured and calculated doses for the 15 MeV beam with phantom A at the plane 1 cm below the ribs slab

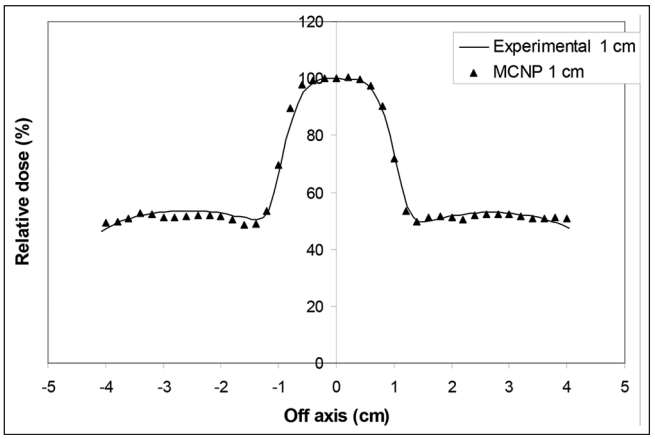

Figure 8: Dose profiles for the 8 MeV beam 1 cm deep under phantom B

values within the air cavity were up to 7% less than the adjacent tissues for the 8 MeV beam and up to 3% less for the 15 MeV beam.

Phantom C

For phantom C, the calculated and measured dose distributions are shown in Figure 10 for both energies. MCNP accurately predicted the dose decrease immediately beyond bone cylinder for the 8 MeV and 15 MeV electron beams. The agreement between measured and calculated doses for the 8 MeV beam is within 1% at most places and within 2% at the edges. The measured and calculated doses agreed within 1.5% for the 15 MeV beam.

Phantom D

Figures 11 and 12 present the results for phantom D irradiated by the 8 and 15 MeV beams. The dose distribution around the inhomogeneity is complicated. For the 8 MeV beam, at a depth of 1 cm under the slab, the calculations are in agreement with the measurements to within 1% except at the cold and hot spots, where the MCNP calculations underestimate measured dose by up to 1.5%. For the 15 MeV beam, the agreement with the measured data is generally within 1.5% and, at the edges of the profile, this agreement is within 2%.

Discussion and Conclusion

The effect of treatment head components

The transport of electrons is dominated by the long-range Coulomb force, resulting in a large number of small interactions. This great increase in computational complexity makes the dose distribution of electron beams more sensitive to collimation than photon beams, because of scatter of the primary electron off the scattering foils, jaws and collimating system as well as the creation of contamination electrons there. MCNP can accurately predict the effects of head components on PDD and Bremesstralung contribution. As can be seen from the results, there is no significant difference between 1° and 27° beam divergence on depth dose, but the monodirectional beam shows a very large difference to them.[21] Bieda *et al.*[23] have stated that the scattering foil design and thickness influence the bremsstrahlung dose, broaden the beam and increase the energy spread at the patient surface, but in this study we found that the first scattering foil (of the actual thickness given by the manufacturer) has no significant effect on the Bremesstralung tail. The reason may be the very small thickness of scattering foil (0.1-1 mm) and also the great distance from the surface of the phantom. In contrast to the first scattering foil, the secondary scattering

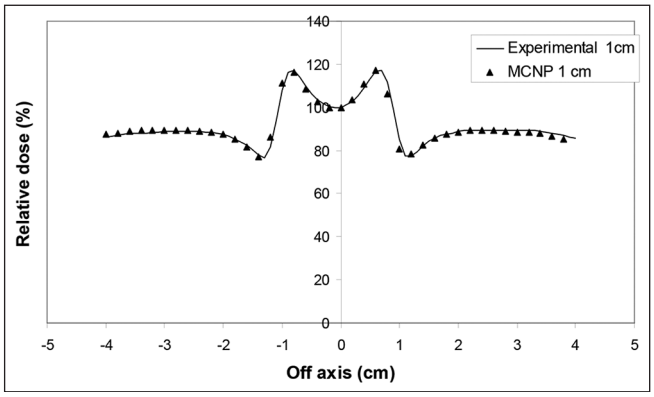

Figure 9: Dose profiles for the 15 MeV beam 1 cm deep under phantom B

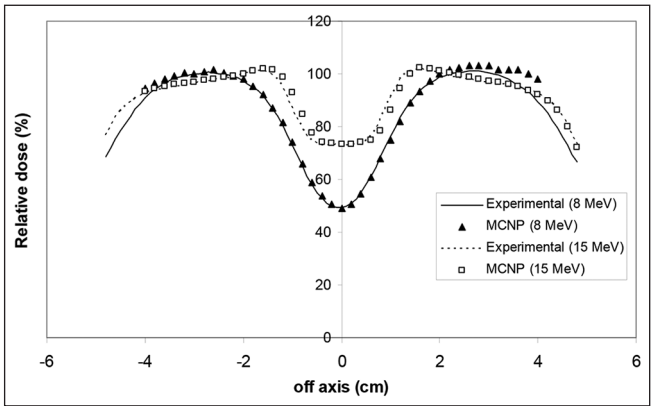

Figure 10: Dose profiles for the 8 MeV and 15 MeV beams 1 cm deep below phantom C

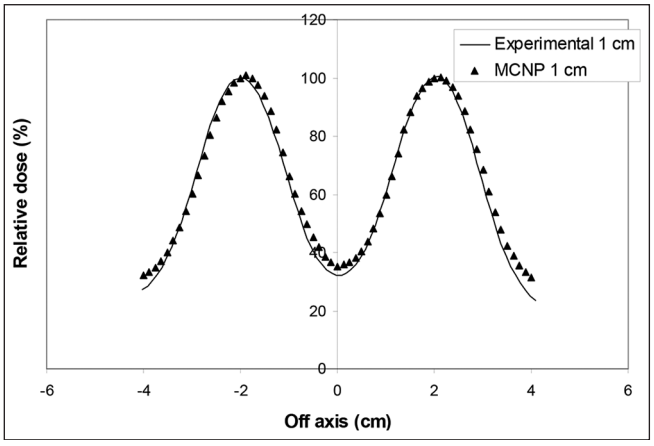

Figure 11: Dose profile 1 cm deep under phantom D for the 8 MeV beam (the started scan point was under the center disk)

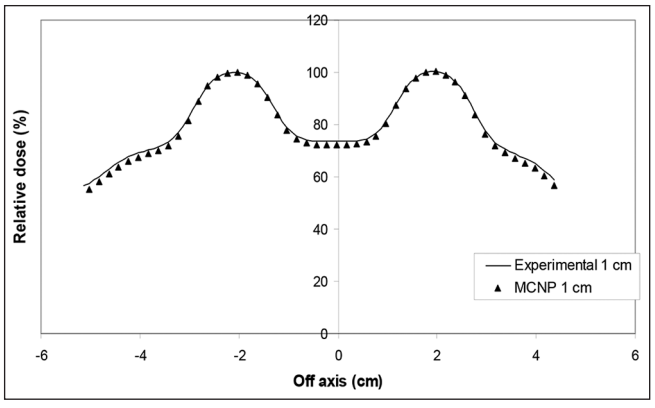

Figure 12: Dose profile 1 cm deep under phantom D for the 15 MeV Beam (the started scan point was under the center disk)

foil, X and Y jaws and electron applicator provide as much as 5% of the dose. Our results also show that a full-component simulation is necessary in order to obtain a realistic model of the beam.

Evaluation of Monte Carlo N Particle in homogenous and inhomogeneous phantoms

On comparing the MCNP results with experimental measurements, good agreement was found in the homogenous phantom. A 2%/2 mm criterion (including both systematic and statistical uncertainty) has been used in the commissioning of MC-based dose calculations.[10,24] In our study, discrepancies in both the energies were within 2% and 2 mm in the homogenous phantom. To obtain a good agreement, the user has to define the geometry, materials and densities accurately and also carry out a "tuning" procedure. Tuning is very important and can be done in two steps:

a. Varying the primary electron energy of a monoenergetic electron pencil beam for a 10 cm × 10 cm field to match the measured dose in the phantom. We found that the depth doses were sensitive to primary electron energy. In our MCNP results, variation of 0.2 MeV showed differences (2-4%) on the PDD curve. Another alternative for varying is using the energy spectrum, which is more reliable in MCNP. Defining the energy distribution at the exit window for one nominal energy is not the same in different MC codes. In our experience with MCNP, the mean energy variation and weights change the position of PDD curve shoulder and bremsstrahlung tail.
b. When the electron energy has been estimated, vary the radial width of a Gaussian electron beam to match the measured dose profiles at a shallow depth. In our experience, the manufacturer's data of full-width-at-half-maximum (FWHM) gave good results with MCNP.

The predictions of MCNP dose calculation in the presence of heterogeneities agree within 3%. Scattered electrons from these media contribute to an increase in dose laterally to each side of the rib (for example) and decrease in dose behind the ribs between 25% and 50% and also increase scattering in the medium itself, which increases the dose in the media. This increased dose is due to increased electron fluence resulting from the increased angulations of the electrons in bone and the increased number of backscattered electrons and delta rays. Scattering effects are seen more severely for 8 MeV than for 15 MeV. At deeper depths under the bone, the degraded doses are compensated by the scattered electrons that are created from adjacent tissues. An advantage of MC calculation is prediction of dose in places where the experimental measurements are impractical or inaccurate due to electron disequilibrium (e.g., inside an inhomogeneity insert).

There are still two limitations in the application of MCNP to computing routine dose distributions in the clinic. The first is run time. Required time for obtaining statistically acceptable results in this study ranged from 65 to 75 h in the homogenous phantom. In the case of heterogeneous phantoms, to obtain the phase space file, the required time was 225 h and to obtain the results from the phase space file, 1/3 of this time was required. If a high degree of accuracy is required, more time for running is unavoidable. There are, however, some techniques for reducing run time, such as energy cut-off and variance reduction methods.

The second problem is the required hard disc space for storing the RUNTPE file and, in the case of phase space file, the W file. In this study, the required space for both files ranged from 750 MB to 1.5 GB for each calculation. This is no longer a problem with the currently available technology.

Results obtained with the MCNP4C agree well with the measured electron dose distributions. We have shown that the results of MCNP in a "complex" phantom are generally within 2% of the measurements for the energies studied, which further suggests the capability of MCNP to model complex geometries. This, combined with its user-friendliness and ability to handle complex geometries, makes MCNP4C an attractive code for electron transport calculations.

Acknowledgments

The authors are grateful to the staff at the Physics Department of the Royal Marsden Hospital, London and Surrey, UK, for their invaluable help.

References

1. Hogstrom KR, Mills MD, Almond PR. Electron beam dose calculations. Phys Med Biol 1981;26:445-59.
2. Ma CM, Faddegon BA, Rogers DW, Mackie TR. Accurate characterization of Monte Carlo calculated electron beams for radiotherapy. Med Phys 1997;24:401-16.
3. Cygler J, Battista JJ, Scrimger JW, Mah E, Antolak J. Electron dose distributions in experimental phantoms: A comparison with 2D pencil beam calculations. Phys Med Biol 1987;32:1073-86.
4. Mah E, Antolak J, Scrimger JW, Battista JJ. Experimental evaluation of a 2D and 3D electron pencil beam algorithm. Phys Med Biol 1989;34:1179-94.
5. Andreo P. Monte Carlo techniques in medical radiation physics. Phys Med Biol 1991;36:861-920.
6. Rogers DW, Faddegon BA, Ding GX, Ma CM, We J, Mackie TR. BEAM: A Monte Carlo code to simulate radiotherapy treatment units. Med Phys 1995;22:503-24.
7. Doucet R, Olivares M, DeBlois F, Podgorsak EB, Kawrakow I, Seuntjens J. Comparison of measured and Monte Carlo calculated dose distributions in inhomogeneous phantoms in clinical electron beams. Phys Med Biol 2003;48:2339-54.
8. Solberg TD, DeMarco JJ, Chetty IJ, Mesa AV, Cagnon CH. A review of radiation dosimetry application using the MCNP Monte Carlo code. Radiochim Acta 2001;89:337-55.
9. Tertel J, Wulff J, Karle H, Zink K. Verification of a commercial implementation of the Macro-Monte-Carlo electron dose calculation

algorithm using the virtual accelerator approach. Z Med Phys 2010;20:51-60.
10. Ma CM, Mok E, Kapur A, Pawlicki T, Findley D, Brain S, *et al*. Clinical implementation of a Monte Carlo treatment planning system. Med Phys 1999;26:2133-43.
11. Halbleib H. Structure and operation of the ITS code system. In: Jenkins TM, Nelson WR, Rindi A, Nahum AE, Rogers DW, editors. Monte Carlo Transport of Electrons and Photons. New York: Plenum; 1988. p. 249-62.
12. Seltzer SM. An overview of ETRAN Monte Carlo methods. In: Jenkins TM, Nelson WR, Rindi A, Nahum AE, Rogers DW, editors. Monte Carlo Transport of Electrons and Photons. New York: Plenum; 1988. p. 153-82.
13. Nelson WR, Hirayama H, Rogers DW. The EGSG4 Code System. Stanford Linear Accelerator Centre (SLAC), Report 265, 1985.
14. Baro J, Sempau J, Fernandez-Vera JM, Salvat F. PENELOPE: An algorithm for Monte Carlo simulation of the penetration and energy loss of electrons and positron in matter. 1 B 1995;100:31-46.
15. Rogers DW, Bielajew AF. Monte Carlo Techniques of electron and photon transport for radiation dosimetry. Ottawa: National Research Council of Canada; 1990.
16. Jeraj R, Keall PJ, Ostwald PM. Comparisons between MCNP, EGS4 and experiment for clinical electron beams. Phys Med Biol 1999;44:705-17.
17. Briesmeister JF. MCNP A General Monte Carlo N particle transport code. Los Alamos national laboratory report. LA- 13709-M, 2000.
18. Ma CM, Jiang SB. Monte Carlo modelling of electron beams from medical accelerators. Phys Med Biol 1999;44:R157-89.
19. Khan FM, Doppke KP, Hogstrom KR, Kutcher GJ, Nath R, Prasad SC, *et al*. Clinical electron-beam dosimetry: Report of AAPM Radiation Therapy Committee Task Group No. 25. Med Phys 1991;18:73-109.
20. Thwaites DI, DuSautoy AR, Jordan T, McEwen MR, Nisbet A, Nahum AE, *et al*. IPEMB Report. The IPEMB code of practice for electron dosimetry for radiotherapy beams of initial energy from 2 to 25 MeV based on absorbed dose to water calibration. Phys Med Biol 2003;48:2929-70.
21. Nedaie HA, Mosleh-Shirazi MA, Shariary M, Gharaati H, Allahverdi M. Monte Carlo study of electron dose distributions produced by the elekta precise linear accelerator. Rep Pract Oncol Radiother 2006;11:287-92.
22. Schaart DR, Jansen JT, Zoetelief J, de Leege PF. A comparison of MCNP4C electron transport with ITS 3.0 and experiment at incident energies between 100 keV and 20 MeV: Influence of voxel size, substeps and energy indexing algorithm. Phys Med Biol 2002;47:1459-84.
23. Bieda MR, Antolak JA, Hogstrom KR. The effect of scattering foil parameters on electron-beam Monte Carlo calculations. Med Phys 2001;28:2527-34.
24. Jiang SB, Deng J, Li JS, Pawlickib T, Boyer AL. Modeling and commissioning of clinical photon beams for Monte Carlo treatment planning. In: Schlegel W, Bortfeld T, editors. In: Proc. 13th Int. Conf. on the Use of Computer in Radiation Therapy. Heidelberg: Springer- Verlag; 2000. p. 434-6.

How to cite this article: Nedaie HA, Mosleh-Shirazi MA, Allahverdi M. Monte Carlo N Particle code - Dose distribution of clinical electron beams in inhomogeneous phantoms. J Med Phys 2013;38:15-21.
Source of Support: Nil, **Conflict of Interest:** None declared.